In-situ incubation of a coral patch for community-scale assessment of metabolic and chemical processes on a reef slope

Steven M.A.C. van Heuven[1,*], Alice E. Webb[1,*], Didier M. de Bakker[2,3], Erik Meesters[3], Fleur C. van Duyl[2], Gert-Jan Reichart[1,4] and Lennart J. de Nooijer[1]

[1] Department of Ocean Sciences, NIOZ Royal Netherlands Institute for Sea Research, and Utrecht University, Den Hoorn, Noord-Holland, The Netherlands
[2] Department of Marine Microbiology, NIOZ Royal Netherlands Institute for Sea Research, and Utrecht University, Den Hoorn, Noord-Holland, The Netherlands
[3] Wageningen Marine Research, Wageningen University and Research, Den Helder, Noord-Holland, The Netherlands
[4] Department of Earth Sciences, Utrecht University, Utrecht, Utrecht, The Netherlands
* These authors contributed equally to this work.

ABSTRACT

Anthropogenic pressures threaten the health of coral reefs globally. Some of these pressures directly affect coral functioning, while others are indirect, for example by promoting the capacity of bioeroders to dissolve coral aragonite. To assess the coral reef status, it is necessary to validate community-scale measurements of metabolic and geochemical processes in the field, by determining fluxes from enclosed coral reef patches. Here, we investigate diurnal trends of carbonate chemistry, dissolved organic carbon, oxygen, and nutrients on a 20 m deep coral reef patch offshore from the island of Saba, Dutch Caribbean by means of tent incubations. The obtained trends are related to benthic carbon fluxes by quantifying net community calcification (NCC) and net community production (NCP). The relatively strong currents and swell-induced near-bottom surge at this location caused minor seawater exchange between the incubated reef and ambient water. Employing a compensating interpretive model, the exchange is used to our advantage as it maintains reasonably ventilated conditions, which conceivably prevents metabolic arrest during incubation periods of multiple hours. No diurnal trends in carbonate chemistry were detected and all net diurnal rates of production were strongly skewed towards respiration suggesting net heterotrophy in all incubations. The NCC inferred from our incubations ranges from −0.2 to 1.4 mmol $CaCO_3$ m^{-2} h^{-1} (−0.2 to 1.2 kg $CaCO_3$ m^{-2} $year^{-1}$) and NCP varies from −9 to −21.7 mmol m^{-2} h^{-1} (net respiration). When comparing to the consensus-based *ReefBudget* approach, the estimated NCC rate for the incubated full planar area (0.36 kg $CaCO_3$ m^{-2} $year^{-1}$) was lower, but still within range of the different NCC inferred from our incubations. Field trials indicate that the tent-based incubation as presented here, coupled with an appropriate interpretive model, is an effective tool to investigate, in situ, the state of coral reef patches even when located in a relatively hydrodynamic environment.

Subjects Biodiversity, Ecology, Marine Biology
Keywords Coral reef, Incubation, Alkalinity anomaly

Submitted 4 April 2018
Accepted 18 October 2018
Published 3 December 2018

Corresponding author
Lennart J. de Nooijer,
ldenooijer@nioz.nl

Academic editor
Craig Nelson

Additional Information and Declarations can be found on page 18

DOI **10.7717/peerj.5966**

How to cite this article van Heuven SMAC, Webb AE, de Bakker DM, Meesters E, van Duyl FC, Reichart G-J, de Nooijer LJ. 2018. In-situ incubation of a coral patch for community-scale assessment of metabolic and chemical processes on a reef slope. **PeerJ 6:e5966 DOI 10.7717/peerj.5966**

INTRODUCTION

The functionality of many reef systems is intrinsically linked to their structural habitat complexity (*Newman et al., 2006*; *Graham & Nash, 2013*; *Kennedy et al., 2013*). On tropical coral reefs, the three-dimensional habitat relies primarily on the ability of corals to deposit large quantities of calcium carbonate. Over recent decades, corals reefs have been under threat at a global scale by a large number of anthropogenic impacts such as ocean warming, overfishing, eutrophication, and ocean acidification (*Hoegh-Guldberg, 1999*; *Gardner et al., 2003*; *Hoegh-Guldberg et al., 2007*; *De'ath et al., 2012*; *Anthony et al., 2008*; *Baker, Glynn & Riegl, 2008*).

The consequential decline in coral cover and the reduction in historically dominant framework building coral species has already resulted in a substantial loss of 3D-complexity on many tropical reefs (*Edinger & Risk, 2000*; *Alvarez-Filip et al., 2011a*; *Perry et al., 2015*; *De Bakker et al., 2016*; *Hughes, 1994*; *Hughes et al., 2007*).

The impact of individual aspects of environmental change on coral reef health has been assessed in a number of laboratory experiments (*Gilmour, 1999*; *Burkepile & Hay, 2009*). However, in situ community-scale measurements of metabolic and geochemical processes would enable characterization of total reef metabolism. Net community calcification (NCC) is considered to reflect the overall response of the community to environmental change and is therefore monitored as a proxy for coral reefs' status (*Gattuso et al., 1993*; *Kleypas et al., 1999*; *Edinger et al., 2000*). Field validation of coral accretion/decline is required to test whether observed experimental responses can be translated to whole ecosystems and in situ conditions. Coral reef decline or community compositional change can be estimated qualitatively from visual inspection of the same site over time (*Aronson & Precht, 1997*), or by digital comparison of photographs taken at intervals (*Porter & Meier, 1992*; *Coles & Brown, 2007*; *De Bakker et al., 2016*). The disadvantage of such visual assessments, however, is that results are confined to areas that have been visited previously and are not quantitative with respect to NCC. Still, the latter may be estimated from visual inspections using typical, species-specific calcification rates (*Perry, Spencer & Kench, 2008*). And although demonstrated to have fair accuracy (*Porter & Meier, 1992*; *Alevizon & Porter, 2015*; *Chow et al., 2016*), "carbonate budgeting" estimates do not allow estimating seasonal variability of NCC (*Courtney et al., 2016*), and are inherently insensitive to rapid environmental change. The same goes for elevation-change analyses using coral cores as alone do not relate alteration in seafloor structure to cause (*Hubbard, Miller & Scaturo, 1990*; *Yates et al., 2017*). Furthermore, the integrated effects due to organismal interactions cannot be assessed with such an approach. For example, ocean acidification may reduce coral NCC (*Andersson & Gledhill, 2013*) and at the same time increase erosion rates by sponges (*Fang et al., 2013*; *Webb et al., 2017*). Census approach has yet to include the role of several bioeroders (excavating sponges) (*Murphy et al., 2016*), which have been observed to become increasingly dominant on Caribbean reefs (*Chaves-Fonnegra, Zea & Gómez, 2007*). Moreover, ongoing ocean acidification appears to promote the contribution of chemical $CaCO_3$ dissolution to total bioerosion by sponges even further (*Duckworth & Peterson, 2013*; *Wisshak et al., 2013*). Lastly, *Silbiger & Donahue (2015)*

suggest that, under future climate conditions of increased pCO_2 and ongoing warming, dissolution of existing reef carbonates is likely to be more affected than the growing of new reefs as such. Together this implies that there is an urgent need for in situ determination of NCC at the ecosystem level.

Direct approaches to accurately quantify NCC generally rely on determining the flux of alkalinity between water column and reef (*Smith & Key, 1975*). For reefs in environments characterized by a relatively linear flow of water over the reef, the upstream/downstream method (*Odum & Hoskin, 1958*; *Gattuso et al., 1996*) can be employed to determine NCC (*Shaw et al., 2014*; *Koweek et al., 2015*; *Albright et al., 2016*). For less unidirectional flow regimes, estimates based on overall residence time and knowledge of offshore conditions is needed (*Courtney et al., 2016*). In environments where low turbulence allows buildup of appreciable chemical vertical gradients, these gradients have been used to calculate net fluxes (*McGillis et al., 2011*; *Takeshita et al., 2016*). For fully exposed reefs, where no measurable accumulation may occur even in the boundary layer, the use of incubators is necessary. Several such incubation methods have been designed and applied. Most incubators cover a limited area (*Patterson, Sebens & Olson, 1991*; *Haas et al., 2013*; *Camp et al., 2015*), allowing single-species incubations. In most cases, numerous incubations are necessary to accurately capture variability between different locations on a reef in accretion/erosion and thus accurately estimate whole ecosystem NCC. When employing small-volume incubators, care must also be taken to maintain representative hydrodynamic conditions for the incubation species. Moreover, incubations must be terminated before NCC becomes depressed (for example by depletion of oxygen). Larger incubation structures (*Yates & Halley, 2003*) better capture variability on a community scale and convey environmental hydrodynamic conditions (surge) which, on the other hand, may cause inadvertent leakage of enclosed water. This potential exchange between ambient and enclosed water complicates the interpretation of observed chemical changes, particularly for signals that take relatively long to manifest themselves (e.g., alkalinity). The latter limitation restricts this method into hydrodynamically favorable (i.e., calm) conditions (*McGillis et al., 2011*). Additionally, due to obvious logistical challenges, most or all in situ incubations have been carried out on the reef flat.

Here, we aim to assess diurnal coral reef metabolic rates by investigating the in situ inorganic carbonate system over a reef slope coral reef patch offshore from the island of Saba, Dutch Caribbean. We use a tent-based incubation system in an environment with relatively strong currents and swell-induced near-bottom surge that caused modest exchange between the incubated reef and ambient water. Exchange between the enclosed and surrounding seawater is used to our advantage as this maintains oxygenated conditions during the incubation, thus allowing for increased incubation periods. Precise monitoring of temperature and salinity, both inside and outside the tent, allows for accurate determination of the amount of exchange across the enclosure. Explicitly accounting for the role of ambient variability, the benthic fluxes originating within the tent are inferred with high accuracy. Comprehensive monitoring of CO_2 system parameters (dissolved inorganic carbon, total alkalinity), dissolved oxygen, and nutrients (phosphate, nitrate, nitrite, and ammonium) allows for subsequent quantification of integrated

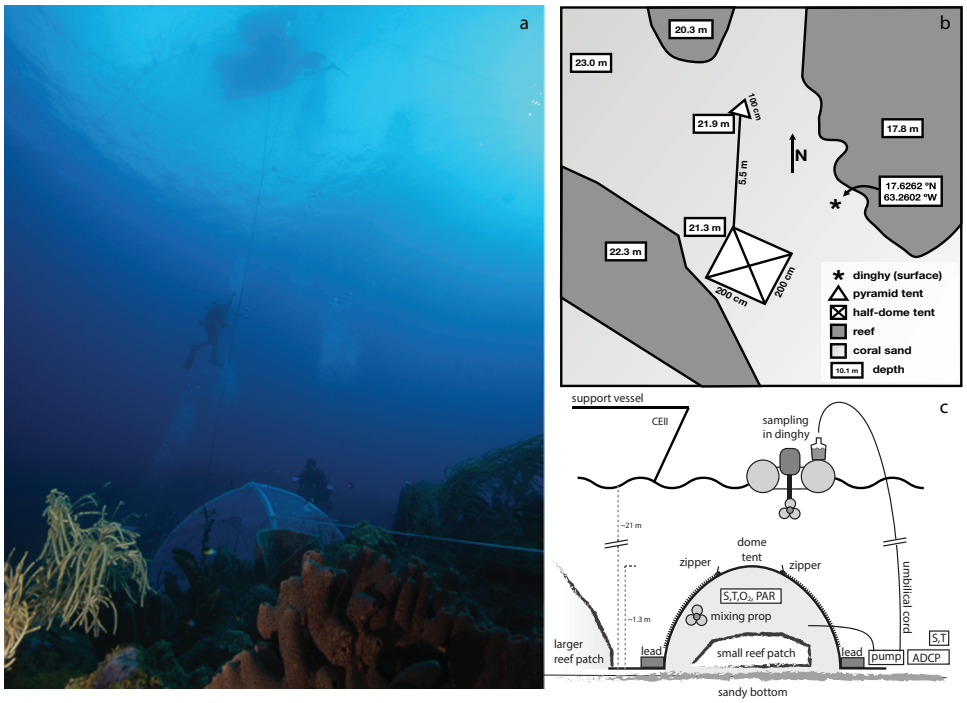

Figure 1 Area where the experimental enclosure was achieved with a schematic outline of the tent incubation. (A) Photograph depicting tent, umbilical cord, support divers, and the dingy used for sample collection. (B) Schematic layout of the tent and surroundings. The Island of Saba is located to the east of this location. (C) Schematic side view of the employed setup for enclosure of a small patch of coral reef. The central structure is a rigid, inflatable dome tent, held securely in place by lead bricks and guy-lines (not shown). Inside the tent are located a battery powered mixing propeller for maintaining water circulation, and analyzers for salinity (S), temperature (T), oxygen (O_2), and PAR. External to the enclosure are located another S/T analyzer, a current profiler and a pump (powered intermittently from the surface) which through an umbilical cord delivers enclosure interior water to the sea surface for sampling. Sampling of exterior water was performed either by this pump (with SCUBA divers temporarily disconnecting the connection to the tent interior) or by divers using large volume syringes. Zippers allow for opening of tent windows for re-equilibrating interior and exterior conditions between incubations. Full-size DOI: 10.7717/peerj.5966/fig-1

whole ecosystem coral reef metabolic processes (NCC and net community production) in a highly hydrodynamic environment.

METHODS

Site and substrate

Reef incubations were performed west of the island of Saba in Ladder Bay at the Ladder Labyrinth mooring site of the Saba National Marine Park (17.6261°N, 63.2602°W) (Field permit approved by the Dutch Ministry of Infrastructure and Environment: RWS-2015/38370), between October 26th and 29th 2015, at a depth of 21 m (Fig. 1). The reef in this area has a distinct spur-and-groove morphology, and is located on a steep incline from the heights of Saba toward the ~500 m deep stretch between the island and the Saba Bank carbonate platform. Coral reefs around Saba harbor a relatively rich diversity of marine species in the context of the wider Caribbean (*Etnoyer, Wirshing & Sanchez, 2010*). The location at which the tent was placed, was chosen such that a patch of

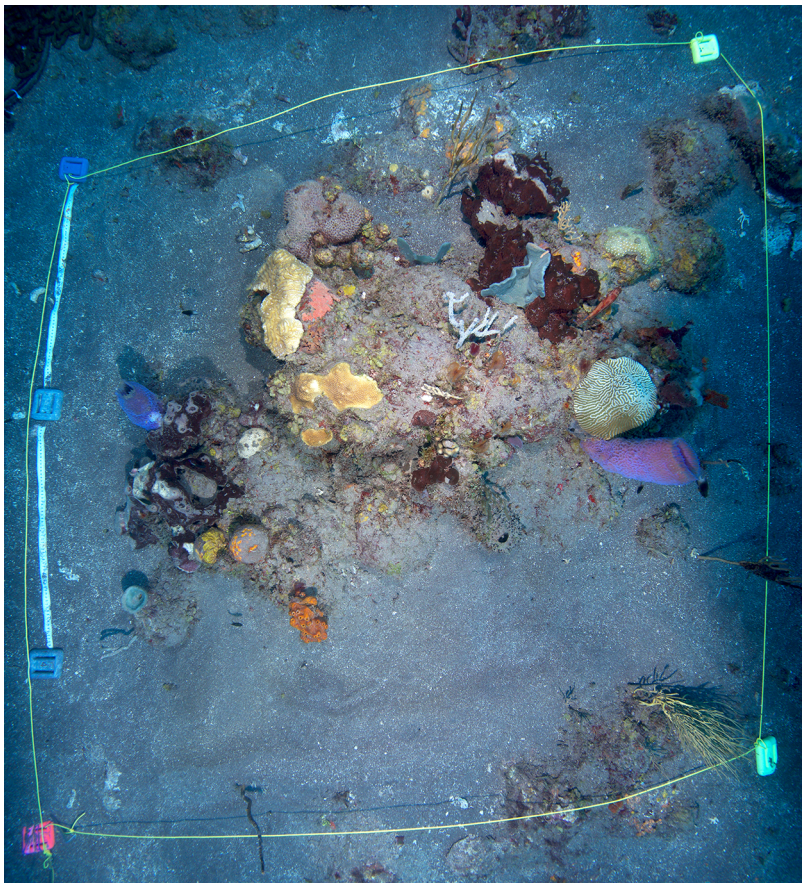

Figure 2 Overview of the enclosed coral patch, after removal of tent at end of experiment. Overview of the enclosed coral reef patch, after termination of the tent incubation. Yellow lines mark the extent of the tent (approximately 2 × 2 m). Full-size DOI: 10.7717/peerj.5966/fig-2

coral reef with a community representative of the wider area was fully enclosed (Fig. 2). Within the 2 × 2 m enclosure, one larger and several smaller carbonate structures were present, acting as main substratum for benthic biota, together resulting in a in a total hard surface area ~4.4 m^2 and a 14% surface enlargement (rugosity). Abiotic components (sand and bare rock) accounted for 61% of the total surface area within the enclosure. Algae (algal turf, *Lobophora* spp., *Dictyota* spp.) covered 22%, sponges (among others *Agelas* sp. and *Callyspongia plicifera*) covered 7% and calcifying species such as corals (including *Orbicella faveolata*, *Meandrina meandrites*, and *Diploria clivosa*) and crustose coralline algae covered 4.2, and 6.6% of the total surface area, respectively (Fig. 2). No macro-bioeroding organisms were visible. A small number of heterotrophic animals, including small fish, crustaceans, and nudibranch, were present during the time of the incubation.

Enclosure

The incubation enclosure is a custom-made, semi-hemispherical, bottomless, transparent dome tent with a square, four m^2 footprint and ~3.2 m^3 volume. The tent walls consist of transparent polyvinylchloride of 0.8 mm thickness, with nontransparent reinforcements

Table 1 Timing of the five incubations.

Incubation	1	2	3	4	5
Latitude	17.6261°N				
Longitude	63.2602°W				
Depth (m)	21				
Start (local time)	October 27, 09:17	October 27, 17:10	October 28, 08:33	October 28, 17:15	October 29, 08:10
End (local time)	October 27, 14:59	October 27, 22:13	October 28, 14:47	October 28, 23:20	October 29, 16:10
Duration (min)	342	303	374	365	480
Light mean (PAR)	65	3	58	3	91
Std	23	1	14	1	15
Minimum	22	2	11	2	5
Maximum	120	8	75	8	161

Note:
Incubation starting and end times, duration, and light. The listed PAR values are in µmol quanta m^{-2} s^{-1}.

along the edges. The tent was inflated (on sandy sediment) by pumping water into the ribs of the dome, after which the rigid tent was carefully moved in place over the coral mound. Flaps extended ~50 cm outward from each of the tent's four sides, allowing for proper sealing of the tent to the substrate by placing weights on the flaps. All four sides of the tent contained an opening of ~0.3 m^2 to allow flushing of the enclosed volume between incubations: during each incubation this opening was sealed. Water enclosed in the incubation tent was homogenized by a continuously running propeller pump (model PP20; Jebao Ltd., Zhongshan, China). This pump was positioned close to one of the tent arches, at half the height of the tent, and generated a slight circulating turbulence, while minimizing stirring up of sediment. Effectiveness of the stirring was demonstrated by rapid and even dispersal of a small dose of injected fluorescein. Time required for initial deployment of the tent was approximately 4 h. In total, five incubations were carried out on this location, three during the day (incubations 1, 3, and 5) and two at night (incubations 2 and 4) (Table 1).

On the sandy substrate, adjacent to the main tent, a small secondary incubator was deployed. Its design is tetrahedron-shaped, and features transparent PVC-walled, rigid edges of one m, with 0.5 m long flaps extending from bottom edge. It covers a 0.43 m^2 planar surface, and encloses a 118 l volume, resembling the cBIT described by *Haas et al. (2013)*. Due to equipment constraints, only limited monitoring of this "sediment blank" incubator was performed by determining the total alkalinity (A_T), total dissolved inorganic carbon (C_T), and nutrient concentrations.

In situ measurements

Measurement of salinity (S), temperature (T), dissolved oxygen (O_2), photosynthetically active radiation (PAR) and water current conditions within the large dome-shaped tent were performed throughout the duration of the incubations (4 h). S, T, and O_2 were measured at 1 min interval using an actively pumped SBE37 MicroCAT equipped with an SBE63 optical dissolved oxygen sensor (Sea-Bird Scientific Inc., Bellevue, WA, USA). Drift of the involved sensors over the duration of our experiment was negligible, while

precision ($\pm 1 \times 10^{-5}$, $\pm 1 \times 10^{-4}$ °C, ± 0.2 μmol kg^{-1}, respectively) is orders of magnitude better than the changes in S, T, and O_2 observed during incubations. PAR was assessed by an Odyssey light logger (Dataflow Systems PTY Ltd., Christchurch, New Zealand), calibrated in air against a superior instrument (Walz ULM500; Walz GmbH, Effeltrich, Germany). The MicroCAT and light logger were suspended from the apex of the enclosure at approximately half the tent's height. A second CTD unit (model CastAway; YSI Inc., Yellow Springs, OH, USA) was deployed outside the tent to register ambient S and T during two out of the five incubations, due to logistical constraints.

Discrete sampling

During incubations, discrete samples were collected every 2 h for analysis of A_T, C_T, total organic carbon (TOC) and nutrients by pumping seawater from the tent interior (and, alternatingly, the exterior) up to the support vessel through a 50 m long 1/4″ Dekabon gas-impermeable "umbilical cord" (Fig. 1). The total volume pumped upward was ~2 l per sampling event, after appropriate flushing (~2 l) of the umbilical (internal volume ~0.5 l).

Most analyses for A_T were performed on-board (*Caribbean Explorer II*) using spectrophotometrically guided single-step acid titration (*Liu et al., 2015*). Additional samples for A_T and C_T were poisoned with $HgCl_2$ immediately after collection (following *Dickson, Sabine & Christian, 2007*) for post-cruise analysis on a VINDTA 3C instrument (*Mintrop et al., 2000*). Accuracy of both instruments was set using certified reference material (batch 144) supplied by Scripps Institute of Oceanography (*Dickson, Sabine & Christian, 2007*). No appreciable bias in A_T was apparent between the two instruments. On the VINDTA, a total of ~125 samples were analyzed for C_T and A_T. Precision of replicates from the same sample bottle was 1.5 μmol kg^{-1} for C_T and 1.0 μmol kg^{-1} for A_T (for both instruments). However, precision for field replicates (i.e., replicates from separate bottles; $n = 23$) was 3.5 μmol kg^{-1} for C_T and 5.0 μmol kg^{-1} for A_T, possibly reflecting suboptimal sampling conditions and/or procedures (e.g., insufficient pre-flushing of umbilical before commencing filling of 1st replicate sample).

Samples for TOC determination were stored in pre-combusted 60 ml EPA vials and acidified and preserved with 8M HCl prior to shore-based analysis on a Shimadzu TOC-V_{CPN}. Analytical precision for TOC (defined as standard deviation of differences between replicates) was ±9.9 μmol kg^{-1} ($n = 8$).

Samples for dissolved inorganic macronutrients (NO_2+NO_3, NO_2, PO_4, and NH_4) were prepared by dispensing sampled water through 0.8/0.2 μm Acrodisc filters into five ml "pony vials," and subsequently stored at −80 °C for later analysis at NIOZ on a QuAAtro continuous flow analyzer (SEAL Analytical GmbH, Norderstedt, Germany) following GO-SHIP protocol (*Hydes et al., 2010*). Uncertainty of nutrient determinations (±0.1, ±0.01, ±0.005, and ±0.005 μmol kg^{-1}, respectively) was substantially smaller than the differences observed between samples taken over the incubation period.

Release of nutrients during respiration decreases A_T (or increases A_T for release of NH_4^+), confounding the interpretation of changes in A_T to represent $CaCO_3$

dissolution only. Following common protocol, we correct calculated A_T for nutrient release as follows:

$$A_T^{obsNC} = A_T^{obs} + PO_4 + NO_3 - NH_4.$$

Throughout the remainder of the manuscript, A_T equals A_T^{obsNC} as defined above.

Outline of data processing

After data collection, a six-step approach was taken to infer fluxes from the measurements. Numbered steps are discussed in more detail in the following sections. Briefly, (1) the leak rate of the enclosure is inferred from measurements of S and T performed simultaneously inside and outside the tent during two of the five incubations. (2) Assuming the inferred leak rate to be valid throughout the experiment (i.e., for the other three incubations as well), time series of exterior S and T are inferred for all incubations from tent interior S and T. (3) Time series of ambient concentrations of C_T, A_T, and O_2 are predicted from linear relationships with salinity. (4) We calculate, accounting for leakage at a known and assumed constant rate, the time rate of substance input into the tent interior that best reproduce the observations made inside the enclosure. (5) We apportion the input of C_T and A_T into the contributions by the processes of $CaCO_3$ dissolution and respiration. Lastly (6), all substance input rates are converted to fluxes.

(1) Rate of water exchange

The rate of water exchange across the enclosure f (in units of min^{-1}) was estimated from the dampened response of measured in-tent salinity (S) to the variability of measured ambient (i.e., outside the tent) salinity over the duration of an incubation. This was performed by iterative minimization (based on least squares) of the residuals *q* in Eq. (1).

$$S_{in}^{calc}{}_{t+1} + q = \left((1 - f) \cdot S_{in}^{calc}{}_{t} + f \cdot S_{ambient\ t}^{meas}\right) - S_{in}^{meas} \quad (1)$$

where, $S_{in}^{calc}{}_{t\,+\,1}$ is the calculated salinity inside the tent at time $t + 1$, $S_{in}^{calc}{}_{t}$ the calculated salinity inside the tent at time t and $S_{ambient\ t}^{meas}$ the measured salinity outside the tent at time t.

(2) Ambient hydrography

With the estimated leak rate estimate *f*, an approximation of ambient salinity $S_{ambient}^{meas}$ may be obtained from S_{in}^{meas}, which is available for all five incubations.

(3) Ambient chemistry

In order to know, at high temporal resolution, the concentrations of O_2, C_T, and T_A outside the enclosure, we regress measurements of these parameters against $S_{ambient}^{calc}$. We use data collected (i) locally at the enclosure, supplemented by data obtained (ii) by vertical profiling down to ~75 m in the vicinity of the incubator and (iii) during expedition PE414 of the Dutch RV Pelagia in Aug/Sep 2016 close to Saba (hydrographic station #49, <5 km from enclosure location; L. J. de Nooijer & S. M. A. C van Heuven, 2017, unpublished data). The use of data collected nearly a year later might be considered

inappropriate. However, comparison between (i) Pelagia and (ii) tent ambient A_T and C_T data (and near tent profiles) is rather favorable.

(4) Time rate of substance input *R*

Having inferred (i) the (assumed constant) rate of exchange of water between tent and environment and (ii) the time history of ambient concentrations C_{out} of the parameter of interest (i.e., A_T, C_T, etc.) next we subsequently determined the constant time rate of substance input R (in $\mu mol\ kg^{-1}\ h^{-1}$) that best explains the observed changes of concentration C_{in} inside the enclosure while accounting for constant exchange with the environment. This is performed through iterative minimization of the residuals q in Eq. (2).

$$C_{in}^{t} + q = C_{in}^{t-1} \cdot (1 - f) + C_{ambient}^{t-1} \cdot f + R \quad (2)$$

The inferred input rate R is somewhat sensitive to the choice of the initial interior concentration ($C_{in}^{t=0}$). Using the measurement collected at the start of the incubation may affect the result due to stochastic measurement error. Therefore we used an initial C_{in} through careful observation of initial measurements performed in the enclosure and of the measured (and predicted) ambient conditions. The dictated initial interior concentrations were identical for all five incubations, supported by the observation of comparable ambient salinity at the start of each incubation.

An estimate of the robustness of the input rates of O_2, C_T, and A_T is obtained using a Monte Carlo approach (Fig. S1). A thousand curve fits were performed as above, but after randomly perturbing (i) each of the measured values of C_T and A_T (both by samples from a normal distribution of widths' of four $\mu mol\ kg^{-1}$, representing the measurement precision), (ii) the times of collection of the samples (s = 5 min) and the leak rate of the tent (s = 0.1% min^{-1}). If the standard deviation of the 1,000 obtained input rates was smaller than the calculated nominal input rate, this nominal rate is considered to be significantly different from zero.

(5) $CaCO_3$ dissolution and respiration rates

As outlined above, measurements of A_T haven been adjusted for the effect of nutrient release by respiration. Subsequently, the individual contributions of $CaCO_3$ dissolution and respiration to the observed concentrations (or fluxes) of A_T and C_T were calculated:

$\Delta A_T^{diss} = \Delta A_T^{obsNC}$	change in A_T due to dissolution
$\Delta A_T^{resp} = 0$	change in A_T due to respiration
$\Delta C_T^{diss} = \Delta A_T^{obsNC}/2$	change in C_T due to dissolution
$\Delta C_T^{resp} = \Delta C_T^{obs} - \Delta C_T^{diss})$	change in C_T due to respiration

(6) Conversion to fluxes

The input rates R (again, in $\mu mol\ kg^{-1}\ h^{-1}$) in the tent are converted to fluxes ($\mu mol\ m^{-2}\ h^{-1}$), assuming an enclosed mass of water of 3,000 ± 150 kg (approximately

3,200 l enclosed; substrate volume is ~250 l; seawater density ~1,022 kg m^{-3}) and an incubated planar surface of 4.4 m^2.

Lastly, we compare our results with NCC estimates based on observed community composition and data published for the fluxes of various classes and species of reef organisms, following the *ReefBudget* approach of *Perry, Spencer & Kench (2008)*. To measure the species-specific cover within the incubated area, we took multiple photos from different angles and then used ImageJ v1.51j8 to quantify the precise cover of each functional benthic group. Rugosity was measured from four crossed transects through the incubated patch (see Tables S1–S3).

RESULTS

Application of Eq. (1) to data collected during incubations four and five yields a leak rate of the enclosure f of ~0.007 min^{-1}. This indicates that ~25 kg of seawater (i.e., 0.007 × 3,000 kg) is exchanged every minute between the incubation enclosure and the environment. Although f ~0.007 accurately relates interior and ambient salinity observations made during incubations 4 and 5, we have no direct means of ascertaining that it also applies to preceding incubations. However, given the sparse ambient salinity data, we assume this water exchange rate to be constant throughout all incubations. Because the sealing of the tent to the substrate remained unchanged from the second incubation onward, the time history of ambient salinity S_{out}^{calc} was derived under the assumption of f being ~0.007. During incubations the error between S_{out}^{meas} and S_{out}^{calc} was –0.023 ± 0.19 (range: 34.7–36.0). The good match indicates validity of this simple adjective exchange model.

The ambient hydrographic conditions reflect variable admixture of a deeper, colder, and more saline component into the warmer, and fresher waterbody that is more commonly encountered at the incubation site (see Fig. 3A). In these ambient waters, C_T and A_T increase with S as is expected. Oxygen, too, is observed to increase with increasing S, due to the higher solubility in the more saline and—crucially—colder water. Regressions between S and $O_2/C_T/A_T$ are presented in Fig. 3, panels B, D, and F. The time histories of these properties, derived using $S_{ambient}^{calc}$ are presented in Fig. 3, panels C, E, and G. For nutrients, no regressions were performed since ambient concentrations were essentially invariant at zero compared to the in-tent changes during incubations (Fig. S2).

Figure 4 illustrates the results of our approach for incubation 4. For an overview of all results from all incubations, please refer to Table S4 and/or Fig. S3. The model employed fits the measurements for C_T and A_T relatively well: the RMSE of the fit of C_T is 3.5 μmol kg^{-1}—identical to the measurement uncertainty of C_T itself. For A_T the fit (5.3 μmol/kg) is slightly worse than instrument precision (3.5 μmol kg^{-1}).

For the five incubations, consumption of oxygen from the incubated seawater ranged from −10 to −30 μmol $kgSW^{-1}$ h^{-1} (Table S4). Concomitant increase of C_T, PO_4, and NO_{2+3} strongly suggests respiration to be the dominant process throughout these incubations. Respiration should decrease A_T slightly due to the release of nutrients, but an even larger decrease is inferred by the full model suggesting a significant role for net calcification during incubation 2, 3, and 4. For the incubation 1 and 5 on the other hand, slight $CaCO_3$ dissolution is inferred. Prior to inferring rates, values of A_T were adjusted

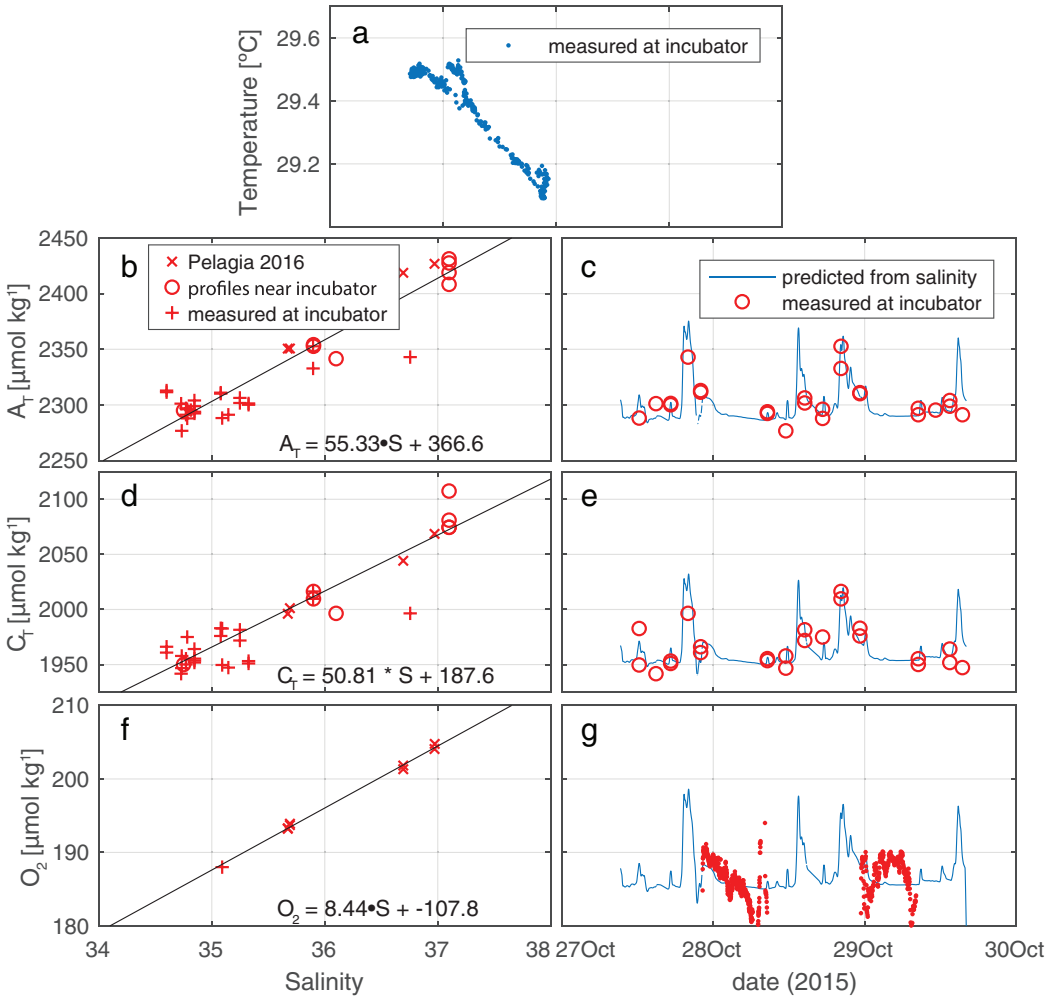

Figure 3 Measured conditions within and outside the tent. (A) Salinity and temperature recorded outside the enclosure show occasional mixing of a cool, saline deep water body into the warmer, fresher surface water component that is most commonly observed at the depth of the enclosure (as indicated by the high density of data points at S~34.8). (B, D, F) Regression against salinity of, respectively, A_T, C_T, and O_2. Samples in these regressions originate from three sources (two for O_2). (C, E, G) Measured values of, respectively A_T, C_T, and O_2, plotted together with time trace of these values, generated from the regressions against salinity. Full-size DOI: 10.7717/peerj.5966/fig-3

to account for the release of nutrients during respiration. Therefore, by definition the respiration A_T rate is zero for all incubations (Table 2).

Results obtained from incubations using the smaller, secondary tent suggests at most a very limited role for sedimentary processes (see Fig. S4): although exterior concentrations of A_T and C_T increased by as much as 60 µmol kg^{-1} in the second half of the incubation, interior A_T and C_T during those 4 h did not increase at rates higher than 2.5 µmol kg^{-1} h^{-1}. This limited response suggests a leak rate between 0.2% and 1% min^{-1}. Appreciable accumulation may therefore be expected if fluxes are present, also because of the small tent's favorable volume-to-surface ratio (275 vs 750 l m^{-2} for the dome tent). Over the first 165 min of the incubation, however, interior A_T and C_T increase only by 1 and 2 µmol kg^{-1} compared to initial conditions (commensurate flux: ~0.3 and 0.6 mmol m^{-2} h^{-1}, that is, one or

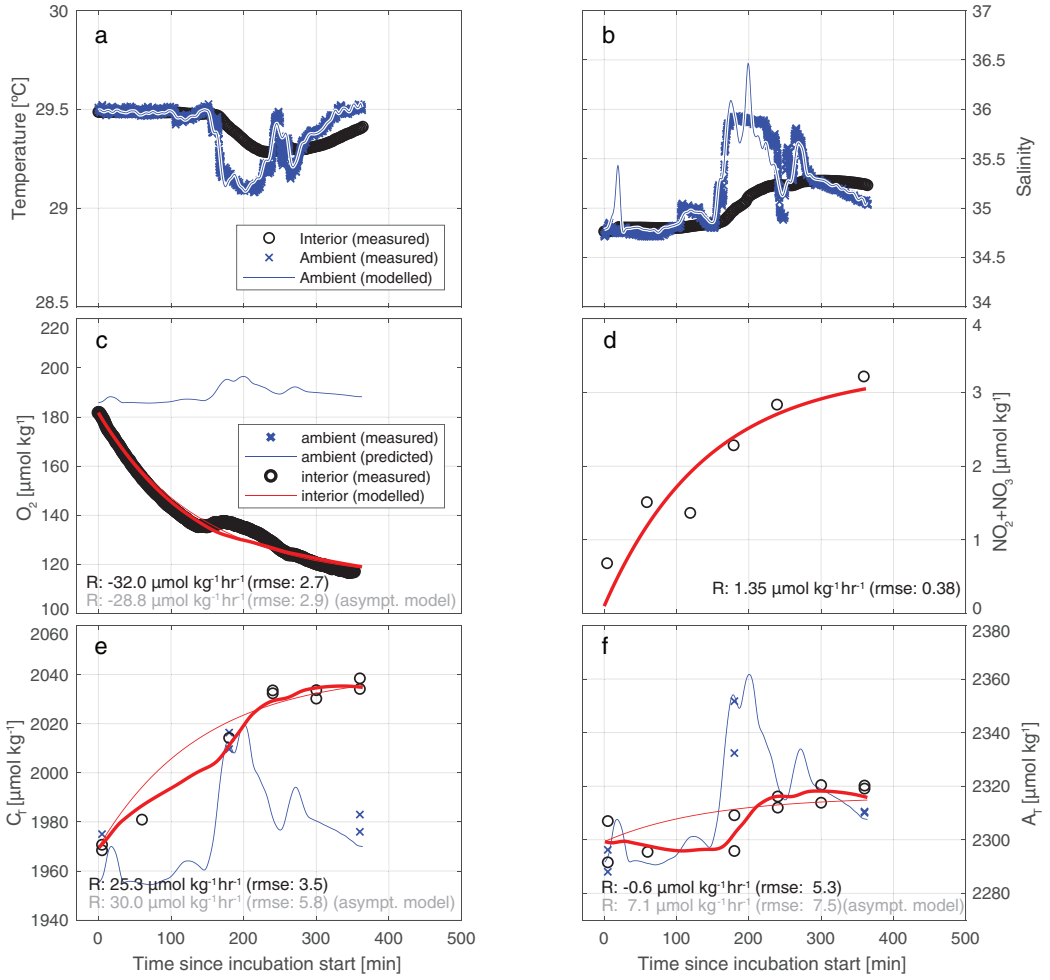

Figure 4 Results of the model employed to infer the input rates from observations. Illustrative results of the model (bold red line) employed to infer the substance input rates from observations, here for incubation 4. The thin blue line depicts the predicted ambient values while the blue crosses represents the measured ambient values. (A) A water exchange rate of 0.007 min^{-1} between enclosure and environment optimally relates ambient and interior measurements of salinity. Back-calculating ambient salinity from interior salinity is shown here to be feasible. (B) Ambient temperature co-varies with S. From T, the exchange rate is inferred to be 0.012 min^{-1} (higher than from S due to additional conductive equilibration). Additionally, in (C–F), we present results of a simplistic asymptotic curve fitting (thin red line) to show how the two methods may diverge appreciably, here mostly evidently for AT. (Note that the uncertainty of the asymptotic fit is worse than that of the model used in this study). Full-size DOI: 10.7717/peerj.5966/fig-4

two orders of magnitude lower than in the main tent; note that appreciable errors apply both to measurements and conversion to flux). These increases may be linked to exchange with ambient waters. No changes in pyramid tent nutrient concentrations were observed, suggesting low rates of productivity or respiratory processes. For subsequent calculations, we consider the contribution by sedimentary processes to be negligible.

Subsequently, the concentration changes in oxygen, inorganic carbon, etc. in the dome-tent were used to calculate the fluxes during each of the five main incubations (Table 2). No trends were observed in TOC concentrations within the tent during incubations, despite clear trends being observed for C_T.

Table 2 Summary of fluxes inferred.

Incubation	1	2	3	4	5
PO_4	0.015 ± 0.004	0.009 ± 0.005	0.016 ± 0.005	0.031 ± 0.009	0.037 ± 0.007
NO_2+NO_3	0.49 ± 0.14	0.55 ± 0.21	0.83 ± 0.09	0.91 ± 0.18	0.81 ± 0.20
NH_4	0.21 ± 1.06	0.26 ± 0.48	0.18 ± 0.05	0.23 ± 0.04	0.17 ± 0.19
NO_2	0.02 ± 0.01	0.01 ± 0.01	0.02 ± 0.00	0.02 ± 0.00	0.01 ± 0.01
SIL	0.44 ± 0.10	0.00 ± 0.18	0.19 ± 0.10	−0.07 ± 0.20	−0.02 ± 0.15
DOC	1.4 ± 4.3	−1.1 ± 4.2	−0.9 ± 4.8	−1.9 ± 2.8	−0.1 ± 5.4
O_2	−9.0 ± 0.7	−13.5 ± 1.1	−13.6 ± 1.3	−21.7 ± 1.9	−17.0 ± 1.6
C_T	5.0 ± 0.8	11.1 ± 1.1	13.0 ± 1.0	17.1 ± 1.6	10.6 ± 1.1
A_T	0.4 ± 0.6	−2.5 ± 0.9	−2.8 ± 0.6	−0.4 ± 0.7	0.4 ± 0.5
C_{Tresp}	4.8 ± 0.8	12.3 ± 1.1	14.4 ± 1.0	17.3 ± 1.6	10.4 ± 1.1
A_{Tresp}	0.0 ± 0.0	0.0 ± 0.0	0.0 ± 0.0	0.0 ± 0.0	0.0 ± 0.0
C_{Tdiss}	0.2 ± 0.3	−1.2 ± 0.4	−1.4 ± 0.3	−0.2 ± 0.4	0.2 ± 0.2
A_{Tdiss}	0.4 ± 0.6	−2.5 ± 0.9	−2.8 ± 0.6	−0.4 ± 0.7	0.4 ± 0.5

Notes:

Summary of fluxes inferred from observed concentration changes in the enclosure during each of five incubation periods. See text for methods for derivation of rates and uncertainties. All fluxes in mmol h^{-1} m^{-2} (planar incubated surface area). Negative dissolution fluxes are described (instead of positive calcification) to maintain co-directionality of the fluxes of respiration and dissolution.

Uncertainties for respiration and dissolution are assumed to be equal to uncertainties in C_T and A_T, respectively.

Deviations of the tent leak rate from the nominal 0.7 % min^{-1} (or "breach events") are observed during all incubations. These deviations from our assumption may negatively affect the inferred rates of change in O_2 concentrations, as evident from the differing slopes of trace and fit near the starts of incubations. Considering only the first 30 min of the oxygen traces (preceding tentative breach events in all incubations), appreciably higher oxygen consumption is inferred than when considering the full traces (Table S5). At constant ambient S, O_2, C_T, and A_T, leakage at a rate higher than the 0.7% min^{-1} that we assume would result in underestimation of the true fluxes of O_2, C_T, and A_T. No change would be observed in the O-flux/C-flux ratio that we infer. Conversely, at times of sudden high ambient S, O_2, C_T, and A_T, leakage at a rate higher than the 0.7% min^{-1} that we assume would result in overestimation of C_T and A_T fluxes, and underestimation of O_2 fluxes. This would change the O-flux/C-flux ratio that we infer. However, as we do not know if the O_2 trace is asymptotic, or that the tent did indeed leak at higher or lower rates than 0.7% min^{-1}, results are likely still valid (i.e., when no breach events occurred, and O_2 deviations resulted from sensor artefacts or true biological activity). We therefore maintained the conceivably affected incubations in the paper.

The NCC inferred from our incubations ranges from −0.2 to 1.2 kg $CaCO_3$ m^{-2} $year^{-1}$ which is on average higher but still in range than the NCC estimated from the *ReefBudget* method (0.36 kg $CaCO_3$ m^{-2} $year^{-1}$, Table 3).

DISCUSSION

Our results indicate that the tent incubation is an effective tool for in situ quantification of reef fluxes in reef-overlaying water. Quantification of fluxes was achieved despite strong

Table 3 Net community calcification estimates from flux-based method and *ReefBudget* method.

Incubation	1	2	3	4	5
$NCC_{(this\ study)}$ (kg $CaCO_3$ m^{-2} $year^{-1}$)	−0.2 ± 0.3	+1.1 ± 0.4	+1.2 ± 0.3	+0.2 ± 0.4	−0.2 ± 0.2
$NCC_{ReefBudget}$ (kg $CaCO_3$ m^{-2} $year^{-1}$)	0.36	0.36	0.36	0.36	0.36
$NCC_{(this\ study)}$ (mmol $CaCO_3$ m^{-2} h^{-1})	−0.2 ± 0.3	+1.2 ± 0.4	+1.4 ± 0.3	+0.2 ± 0.4	−0.2 ± 0.2
$NCC_{ReefBudget}$ (mmol $CaCO_3$ m^{-2} h^{-1})	0.41	0.41	0.41	0.41	0.41

Note:
NCC of the planar total area inside the incubation calculated from fluxes and the *ReefBuget* method.

variability in ambient conditions and in the presence of appreciable swell-induced seawater exchange. To this end we applied a comprehensive conceptual framework for the interpretation of the measured concentration differences. This method allows for a volume exchange between the environment and the incubation thereby replenishing the latter and keeping the O_2 levels within the tent near ambient conditions resulting in minimized unrepresentative reef community metabolism. By continuously monitoring the inside environment and assuming constant exchange rate, fluxes within our incubation can be treated as if acquired by a flow through system. Nonetheless, future application of this or similar incubation methods could be further improved by continuous monitoring of the exchange rate, rather than assuming it to be constant throughout the incubation. This could be obtained for instance by running a second thermosalinograph outside the tent. The application of a conceptually simpler "asymptotic" model yields different and less well-constrained results. Particularly, the direction of the $CaCO_3$ dissolution flux may be seen to be reversed in the simpler method (see also Fig. 4). In all incubations, for both A_T and C_T, the uncertainty in measured concentration differences and the variability between results may be greater for the simpler model (Table S4; Fig. S3). In the case of A_T (Fig. 4F), the assumed-to-be-constant input of A_T inferred by the model applied here is of opposite sign to the simpler asymptotic model result (−0.6 vs +7.1 μmol kg^{-1} h^{-1}). This reversal of sign of the A_T rates observed between the two models (asymptotic and full) is caused by the inability of the asymptotic model to account for occasional intrusion of high-A_T ambient water into the tent during sudden changes in ambient hydrography. The asymptotic model (panels C and D) shows a relatively good fit of the observations of O_2 and NO_{2+3} around the fitted curve, which is due to the invariant ambient concentrations of these parameters.

In contrast with previous studies carried out at shallower depths using either Lagrangian drifts or incubations, all net diurnal rates from this study are strongly skewed toward respiration suggesting net heterotrophy in all incubations. Studies performed at shallower depths shift between net autotroph and net heterotrophy over the course of a day (*Yates & Halley, 2003*; *Albright, Langdon & Anthony, 2013*; *Albright et al., 2015*). However, previously reported average net respiration rates occurring at night on shallower reefs are comparable to results from this study (14.5–35.5 mmol C m^{-2} h^{-1}). Results are also comparable to previously reported values at depth. For example, *Middelburg, Duarte & Gattuso (2005)* compiled a global mean coral reef respiration rate of 131 ± 46 mol C m^{-2} $year^{-1}$. Specifically for their categories "outer reef slopes" and "high activity areas" they report

Table 4 Stoichiometry of rates observed during five incubations.

Incubation	1	2	3	4	5	All	R_{1963}	$A\&S_{1983}$
P	1	1	1	1	1	1	1	1
N	32.8 ± 12.2	61.2 ± 42.1	51.5 ± 17.9	29.7 ± 10.7	21.7 ± 6.5	33.2 ± 5.6	16	30
O	337.5 ± 99.7	1222.4 ± 714.9	805.8 ± 275.4	557.9 ± 175.1	313.3 ± 60.8	535.6 ± 73.3	106	550
C	−608.7 ± 157.5	−1485.3 ± 867.5	−842.9 ± 289.4	−706.6 ± 223.6	−455.2 ± 91.6	−691.7 ± 94.9	−150	−610
O/C	−1.80 ± 0.33	−1.22 ± 0.14	−1.05 ± 0.13	−1.27 ± 0.14	−1.45 ± 0.18	−1.29 ± 0.07	1.22	NA

Note:
Stoichiometry of rates observed during five incubations. Values in column "avg." are calculated as the ratio of the sums of incubations 2–5. Uncertainties are calculated by error propagation. Rightmost two columns show literature values from (i) *Redfield (1963)* and (ii) *Atkinson & Smith (1983)*, representing the elemental compositions of (i) marine phytoplankton and (ii) benthic macroalgae. Our incubation results most closely resemble the latter.

values of 140 ± 70 and 413 ± 187 mol C m^{-2} $year^{-1}$, respectively. This range compares well to the rates reported here (105–298 mol C m^{-2} $year^{-1}$ for the full planar surface). A stoichiometric comparison of the inferred fluxes of C_T, oxygen and nutrients is combined with (i) the canonical "Redfield ratio" (*Redfield, 1963*) of the elemental composition of open ocean phytoplankton and (ii) the median elemental composition of benthic macroalga (*Atkinson & Smith, 1983*), likely resembling the composition of the labile fraction of the locally present organic carbon (Table 4). This shows that the community incubated in this experiment respires carbon and nutrients in a ratio that resembles the composition of benthic macroalgae (*Atkinson & Smith, 1983*) which indicates that the observed signal is indeed originating from the sedimentary, benthic, macrofaunal, and/or bacterial constituents of the enclosed community.

A strong correlation between NCC and net community productivity in reef environments is well documented (*Gattuso et al., 1996*; *Shaw, McNeil & Tilbrook, 2012*; *Shaw et al., 2015*; *McMahon et al., 2013*; *Albright et al., 2015*), however, no correlation was found in our incubations. The NCC inferred from our incubations ranged from −0.2 to 1.2 kg $CaCO_3$ m^{-2} $year^{-1}$ which is on average higher than the mean recorded rate of 0.2 kg $CaCO_3$ m^{-2} $year^{-1}$ associated with a Floridian reef patch (10% coral cover) in shallower waters (*Yates & Halley, 2003*) using a similar method.

Applying the *ReefBudget* approach to our benthic census data for comparison, we obtain a NCC for the full incubated substrate surface (i.e., sand and hard substrate) of ~0.36 kg $CaCO_3$ m^{-2} $year^{-1}$ (see Table 3). This estimate is slightly lower but comparable to the average NCC inferred from our incubations (~0.42 kg $CaCO_3$ m^{-2} $year^{-1}$, Table 3). The range of NCC estimates inferred from our results indicates how sensitive metabolic and chemical processes on coral reefs are to their environment. The chemical flux-based method as presented here is appreciably sensitive to the effects of the surrounding hydrological conditions on the substrate and this may be the source for a slight discrepancy compared to the *ReefBudget* approach. NCC rates acquired by *Perry et al. (2013)* associated with a coral cover ranging between 4% and 5% and at similar depth (17–20 m) in the Bahamas are all negative (ranging from −0.01 kg $CaCO_3$ m^{-2} $year^{-1}$ to −0.23 kg $CaCO_3$ m^{-2} $year^{-1}$). This may be explained by varying community composition such as the absence of macro-bioeroders within our tent. Furthermore, the flux-based method does not assess the mechanical component of

bioerosion (caused by parrot fish or sponges for instance) which is important to the process of reef accretion.

The *ReefBudget* method offers a fast and convenient tool for estimating reef biogenic carbonate production states both on a remarkable temporal and spatial scale. Although the incubated flux-based approach, may be more sensitive to unstable and varying reef states, it cannot offer such a large spectrum of study. However, it provides an assessment of the full community without having to determine calcification/dissolution rates as a function of surface area. This can be very useful to assess the effect of endolithic species or determine the impact that some understudied organism may have on the chemical conditions. For instance, benthic cyanobacterial mats have been shown to proliferate around the islands of Curacao and Bonaire since 2003 (*De Bakker et al., 2017*) and are described to effect pH on a local scale (*Hallock, 2005*; *Paerl & Paul, 2012*). However, close to no records on how these mats may alter reef chemical conditions and subsequently impact the calcifying/bioeroding community are available. Currently, the *ReefBudget* approach relies on various assumptions regarding the calculation of each biological component. As such, the flux-based approach described here should not be regarded as a substitute for survey methods such as the *ReefBudget*, but rather as a complementary tool. Using the flux-based approach, it will become easier to determine missing components and variations in chemical dissolution/calcification on a spatial (e.g., depth) and also smaller temporal scale (i.e., diurnal cycle, seasonality), therewith improving survey based carbonate budget assessments.

To determine if the respiration signal might be an artefact of the incubation treatment, we identify potential causes that may perturb the signal. The estimated contribution by macrofauna such as fish, crustaceans, and nudibranchs to the observed respiration signal is deemed to be negligible: considering a fish mass-specific O_2 consumption rate of ~100 $mgO_2\ h^{-1}\ kg^{-1}$ (*Roche et al., 2013*), and assuming 100 grams of fish to be present in the tent (which is likely a strong overestimate as only very few small fish were observed during incubations), we calculate a contribution to C_T in the incubation of ~0.1 $\mu mol\ kg^{-1}\ h^{-1}$, which is two orders of magnitude smaller than the observed respiration rates of 10–30 $\mu mol\ kg^{-1}$. Additionally, we rule out that "free floating" TOC (e.g., coral exudates) is the material that is respired. While clear fluxes are inferred for C_T, no trends were observed in TOC concentrations within the tent during incubations. Alternatively, no significant depression was observed of average interior TOC values ($84 \pm 9\ \mu mol\ kg^{-1}$, $n = 39$) relative to exterior TOC ($86 \pm 7\ \mu mol\ kg^{-1}$, $n = 8$). Although the tentative drop in TOC resembles the small drop observed in dedicated dissolved organic carbon (DOC) depletion experiments (*De Goeij & Van Duyl, 2007*), the lack of volume flow through the tent means TOC cannot be more than a very minor source of respirable carbon. Absence of depletion of suspended labile TOC notwithstanding, TOC may still play a role in the form of mucus if that is adhered to substrate or incubator, out of reach of sampling but available for bacterial respiration. However, the respiring biomass required for the observed C_T increases is unlikely to be present in the form of bacteria, especially shortly after incubation start. Indeed, *Wild et al. (2004)* show from small-scale incubations that the bacterial degradation of coral mucus, introduced into their incubators (containing only sediment

and water column) at high concentrations, occurs at rates of 0.7–2.1 mmol m^{-2} h^{-1}. That compares to rates around 60–175 mmol m^{-2} h^{-1} observed in our experiment, suggesting remineralization of adhered mucus plays at best a minor role in our incubations, further suggesting the observed fluxes to originate from the macroscopic biotic substrate.

In that category, sponges are the most likely organisms respiring, having appreciable biomass and containing ample energy stores to maintain respiration during the incubation periods, in which only limited amounts of organic carbon are available for filter feeding. *Hadas, Ilan & Shpigel (2008)* report (Red Sea) sponge basal oxygen consumption to be ~50% of consumption featured during full water pumping activity, which means that sponge respiration largely continues even when filter feeding ceases. These authors report a rate of 2.4 μmol O_2 h^{-1} g^{-1} (wet weight). Similarly, *Ludeman, Reidenbach & Leys (2017)* report sponge oxygen consumption (standardized to sponge volume) ranging from 0.3 to 3 μmol h^{-1} ml^{-1}, with strong species dependence. Assuming the higher end of this range applies to the sponges incubated in our experiment (mostly *Agelas* sp., *C. plicifera*), and assuming as much as five kg wet weight of sponge to have been present in the enclosure, we account for ~5 μmol kg^{-1} h^{-1} of the observed rates of ~30 μmol kg^{-1} h^{-1}. Maintained respiration by sponges throughout the series of incubations could be fueled by filter feeding during the ~50% of the time in which the incubator was open to the ambient water. Recent research by *McMurray et al. (2018)* showed that species hosting abundant symbiotic microbes (i.e., high microbial abundance, HMA) primarily consumed DOC, while the diet of species with low microbial abundances (LMA) primarily consisted of detritus and picoplankton. They further pointed out that it remained unknown if DOC released by LMA species could be a source of food for HMA species. The main sponges incubated in our experiment are *Agelas* sp. and *C. plicifera* and represent respectively a HMA and a LMA sponge. We tentatively infer that this may explain partly the observed high respiration rate. Nevertheless, we cannot infer if sponges are able to maintain metabolic balance throughout the incubation period, or that they deplete their stores. Further analyses such as bacterial counts would be needed to answer such questions. From Table 2 we conclude oxygen consumption rate during daytime (incubations 2 and 4) to be lower by ~5 μmol kg^{-1} h^{-1} than night time rates (incubations 3 and 5), hinting at a role of primary producers (corals, CCA, macro and microalgae).

The lack of accumulation of C_T in the secondary, small incubation places our sediment at the very low end of literature values regarding respiration. For example, *Middelburg, Duarte & Gattuso (2005)* report a global mean sediment respiration value of ~8.5 ± 7 mmol C m^{-2} h^{-1} (as approximated from their Figure 11.3). Our observed low values may be reasonable considering the highly hydrodynamic nature of the incubation environment which likely hampers settlement of substantial amounts of organic matter onto and into the sediment. In addition, the volcanic sandy composition of the sediment around Saba may be less prone to dissolution than coralline sediment and could explain the insignificant increase in A_T in the small tent. However, *Eyre et al. (2018)* shows similar results for sediment around Cook Islands which is mostly composed of calcareous fragments (*Wood, 1967*). *Eyre et al. (2018)* shows that dissolution in reef sediment across

different locations around the world is negatively correlated with the aragonite saturation state (Ω_{ar}). Average Ω_{ar} of ambient water around the tent incubation throughout the experiment is calculated to be 3.85 which is more comparable to islands (Bermuda and Tetiaroa) showing accretion in reef sediment. The combined effects of hydrodynamics and sand composition are likely to explain why our results present neither accretion nor dissolution in our tent's sediment.

CONCLUSIONS

Flux-based carbonate budget studies, as presented here, provide quantitative data on the functional state of reefs in terms of biologically driven carbonate production which is particularly sensitive to ambient environmental conditions. As such, they can be particularly useful for temporal studies, especially to reveal not only diurnal and seasonal patterns but also to capture shifts in functionality of reef systems. We incubated a coral reef patch situated in a high-energy environment which caused a limited amount of seawater exchange. Monitoring of conditions within and outside the tent allowed for determination of the exchange rate and thereby allowed for correcting the respiration and calcification rates. Application of this procedure shows that this reef patch is characterized by NCC inside the tent at a rate within range but on average higher than fluxes reported in previous studies for shallower reef systems indicating coherence in our results. However, the range of NCC estimates inferred from our results accounts for the sensitivity of this reef patch to the surrounding environment. Furthermore, the net heterotrophy reported here both during the day and the night differs from studies performed at shallower depths where shifts between net autotrophy and net heterotrophy are observed. Future research may include various types of substrates and comparison between regions with varying water quality.

ACKNOWLEDGEMENTS

The authors are particularly grateful to the captain and crew of *Caribbean Explorer II*, who have been outstandingly helpful and accommodating. We also would like to thank the institutional support of Saba Marine Parks, Caribbean Netherlands Science Institute (CNSI), and Wageningen Marine Research (WMR). Additional gratitude is reserved for Janine Nauw, Johan Stapel, Steve Piontek, and volunteer divers Oscar Bos, Dahlia Hassell, Jarno Knijff, Ewan Tregarot, Lodewijk van Walraven, and Bas Westerhof.

ADDITIONAL INFORMATION AND DECLARATIONS

Funding

The research was funded by the Netherlands Organisation for Scientific Research (NWO), grant 858.14.020. Erik Meesters was financially supported by the Ministry of Agriculture, Nature and Food Quality, program Caribbean Netherlands (BO-43-021.04). The funders had no role in study design, data collection and analysis, decision to publish, or preparation of the manuscript.

Grant Disclosures

The following grant information was disclosed by the authors:
The Netherlands Organisation for Scientific Research (NWO): 858.14.020.
The Ministry of Agriculture, Nature and Food Quality, program Caribbean Netherlands: BO-43-021.04.

Competing Interests

The authors declare that they have no competing interests.

Author Contributions

- Steven M.A.C. van Heuven conceived and designed the experiments, performed the experiments, analyzed the data, contributed reagents/materials/analysis tools, prepared figures and/or tables, authored or reviewed drafts of the paper, approved the final draft.
- Alice E. Webb conceived and designed the experiments, performed the experiments, analyzed the data, contributed reagents/materials/analysis tools, prepared figures and/or tables, authored or reviewed drafts of the paper, approved the final draft.
- Didier M. de Bakker performed the experiments, analyzed the data, contributed reagents/materials/analysis tools, prepared figures and/or tables, authored or reviewed drafts of the paper, approved the final draft.
- Erik Meesters performed the experiments, analyzed the data, contributed reagents/materials/analysis tools, authored or reviewed drafts of the paper, approved the final draft.
- Fleur C. van Duyl conceived and designed the experiments, performed the experiments, analyzed the data, contributed reagents/materials/analysis tools, prepared figures and/or tables, authored or reviewed drafts of the paper, approved the final draft.
- Gert-Jan Reichart analyzed the data, prepared figures and/or tables, authored or reviewed drafts of the paper, approved the final draft.
- Lennart J. de Nooijer conceived and designed the experiments, analyzed the data, prepared figures and/or tables, authored or reviewed drafts of the paper, approved the final draft.

Field Study Permissions

The following information was supplied relating to field study approvals (i.e., approving body and any reference numbers):

Field experiments were approved by the Dutch Ministry of Infrastructure and Environment (registration number RWS-2015/38370).

Data Availability

The following information was supplied regarding data availability:

4TU.Center for Research Data: https://data.4tu.nl/repository/uuid:d7c6503d-cd91-4a8d-8d50-8583dd215a14.

Supplemental Information

Supplemental information for this article can be found online at http://dx.doi.org/10.7717/peerj.5966#supplemental-information.

REFERENCES

Albright R, Benthuysen J, Cantin N, Caldeira K, Anthony K. 2015. Coral reef metabolism and carbon chemistry dynamics of a coral reef flat. *Geophysical Research Letters* **42(10)**:3980–3988 DOI 10.1002/2015GL063488.

Albright R, Caldeira L, Hosfelt J, Kwiatkowski L, Maclaren JK, Mason BM, Nebuchina Y, Ninokawa A, Pongratz J, Ricke K, Rivlin T, Schneider K, Sesboüé M, Shamberger K, Silverman J, Wolfe K, Zhu K, Caldeira K. 2016. Reversal of ocean acidification enhances net coral reef calcification. *Nature* **531(7594)**:362–365 DOI 10.1038/nature17155.

Albright R, Langdon C, Anthony KRN. 2013. Dynamics of seawater carbonate chemistry, production, and calcification of a coral reef flat, central Great Barrier Reef. Biogeosciences **10(10)**:6747–6758 DOI 10.5194/bg-10-6747-2013.

Alevizon WS, Porter JW. 2015. Coral loss and fish guild stability on a Caribbean coral reef: 1974–2000. *Environmental Biology of Fishes* **98(4)**:1035–1045 DOI 10.1007/s10641-014-0337-5.

Alvarez-Filip L, Dulvy NK, Côté IM, Watkinson AR, Gill JA. 2011a. Coral identity underpins architectural complexity on Caribbean reefs. *Ecological Applications* **21(6)**:2223–2231 DOI 10.1890/10-1563.1.

Andersson AJ, Gledhill D. 2013. Ocean acidification and coral reefs: effects on breakdown, dissolution, and net ecosystem calcification. *Annual Review of Marine Science* **5(1)**:321–348 DOI 10.1146/annurev-marine-121211-172241.

Anthony KRN, Kline DI, Diaz-Pulido G, Dove S, Hoegh-Guldberg O. 2008. Ocean acidification causes bleaching and productivity loss in coral reef builders. *Proceedings of the National Academy of Sciences of the United States of America* **105(45)**:17442–17446 DOI 10.1073/pnas.0804478105.

Aronson RB, Precht WF. 1997. Stasis, biological disturbance, and community structure of a Holocene coral reef. *Paleobiology* **23(3)**:326–346 DOI 10.1017/S0094837300019710.

Atkinson MJ, Smith SV. 1983. C:N:P ratios of benthic marine plants. Limnology and Oceanography **28(3)**:568–574 DOI 10.4319/lo.1983.28.3.0568.

Baker AC, Glynn PW, Riegl B. 2008. Climate change and coral reef bleaching: an ecological assessment of long-term impacts, recovery trends and future outlook. *Estuarine, Coastal and Shelf Science* **80(4)**:435–471 DOI 10.1016/j.ecss.2008.09.003.

Burkepile DE, Hay ME. 2009. Nutrient versus herbivore control of macroalgal community development and coral growth on a Caribbean reef. *Marine Ecology Progress Series* **389**:71–84 DOI 10.3354/meps08142.

Camp EF, Krause S-L, Santos LMF, Naumann MS, Kikuchi RKP, Smith DJ, Wild C, Suggett DJ. 2015. The "Flexi-Chamber": a novel cost-effective in situ respirometry chamber for coral physiological measurements. *PLOS ONE* **10(10)**:e0138800 DOI 10.1371/journal.pone.0138800.

Chaves-Fonnegra A, Zea S, Gómez ML. 2007. Abundance of the excavating sponge Cliona delitrix in relation to sewage discharge at San Andrés Island, SW Caribbean, Colombia. *Boletõn de Investigaciones Marinas y Costeras* **36**:63–78.

Chow MH, Tsang RHL, Lam EKY, Ang P. 2016. Quantifying the degree of coral bleaching using digital photographic technique. *Journal of Experimental Marine Biology and Ecology* **479**:60–68 DOI 10.1016/j.jembe.2016.03.003.

Coles SL, Brown EK. 2007. Twenty-five years of change in coral coverage on a hurricane impacted reef in Hawai'i: the importance of recruitment. *Coral Reefs* **26(3)**:705–717 DOI 10.1007/s00338-007-0257-3.

Courtney TA, Andersson AJ, Bates NR, Collins A, Cyronak T, de Putron SJ, Eyre BD, Garley R, Hochberg EJ, Johnson R, Musielewicz S, Noyes TJ, Sabine CL, Sutton AJ, Toncin J,

Tribollet A. 2016. Comparing chemistry and census-based estimates of net ecosystem calcification on a rim reef in Bermuda. *Frontiers in Marine Science* **3**:181 DOI 10.3389/fmars.2016.00181.

De'ath G, Fabricus KE, Sweatman H, Puotinen M. 2012. The 27-year decline of coral cover on the Great Barrier Reef and its causes. *Proceedings of the National Academy of Sciences of the United States of America* **109(44)**:17995–17999 DOI 10.1073/pnas.1208909109.

De Bakker DM, Meesters EH, Bak RPM, Nieuwland G, van Duyl FC. 2016. Long-term shifts in coral communities on shallow to deep reef slopes of Curaçao and Bonaire: are there any winners? *Frontiers in Marine Science* **3**:247 DOI 10.3389/fmars.2016.00247.

De Bakker DM, Van Duyl FC, Bak RPM, Nugues MM, Nieuwland G, Meesters EH. 2017. 40 years of benthic community change on the Caribbean reefs of curaçao and bonaire: the rise of slimy cyanobacterial mats. *Coral Reefs* **36(2)**:355–367 DOI 10.1007/s00338-016-1534-9.

De Goeij JM, Van Duyl FC. 2007. Coral cavities are sinks of dissolved organic carbon (DOC). *Limnology and Oceanography* **52(6)**:2608–2617 DOI 10.4319/lo.2007.52.6.2608.

Dickson AG, Sabine CL, Christian J. 2007. Guide to best practices for ocean CO_2 measurements. PICES Special Publication 3, 191. *Available at https://www.nodc.noaa.gov/ocads/oceans/Handbook_2007/Guide_all_in_one.pdf*

Duckworth AR, Peterson BJ. 2013. Effects of seawater temperature and pH on the boring rates of the sponge Cliona celata in scallop shells. *Marine Biology* **160(1)**:27–35 DOI 10.1007/s00227-012-2053-z.

Edinger EN, Limmon GV, Jompa J, Widjatmoko W, Heikoop JM, Risk MJ. 2000. Normal coral growth rates on dying reefs: Are coral growth rates good indicators of reef health? *Marine Pollution Bulletin* **40(5)**:404–425 DOI 10.1016/S0025-326X(99)00237-4.

Edinger EN, Risk MJ. 2000. Reef classification by coral morphology predicts coral reef conservation value. *Biological Conservation* **92(1)**:1–13 DOI 10.1016/S0006-3207(99)00067-1.

Etnoyer PJ, Wirshing HH, Sanchez JA. 2010. Rapid assessment of octocoral diversity and habitat on Saba Bank, Nehterlands Antilles. *PLOS ONE* **5(5)**:e10668 DOI 10.1371/journal.pone.0010668.

Eyre BD, Cyronak T, Drupp P, De Carlo EH, Sachs JP, Andersson AJ. 2018. Coral reefs will transition to net dissolving before end of century. *Science* **359(6378)**:908–911 DOI 10.1126/science.aao1118.

Fang JKH, Mello-Athayde MA, Schönberg CHL, Kline DI, Hoegh-Guldberg O, Dove S. 2013. Sponge biomass and bioerosion rates increase under ocean warming and acidification. *Global Change Biology* **19(12)**:3581–3591 DOI 10.1111/gcb.12334.

Gardner TA, Cote IM, Gill JA, Grant A, Watkinson AR. 2003. Long-term region-wide declines in Caribbean corals. Science **301(5635)**:958–960 DOI 10.1126/science.1086050.

Gattuso JP, Pinchon M, Delasalle B, Canon C, Frankignouille M. 1996. Carbon fluxes in coral reefs. I. Langrangian measurement of community metabolism and resulting air-sea CO_2 disequilibrium. *Marine Ecology Progress Series* **145**:109–121 DOI 10.3354/meps145109.

Gattuso JP, Pichon M, Delesalle B, Frankignouille M. 1993. Community metabolism and air-sea CO2 fluxes in a coral-reef ecosystem (Moorea, French-Polynesia). *Marine Ecology Progress Series* **96(3)**:259–267 DOI 10.3354/meps096259.

Gilmour J. 1999. Experimental investigation into the effects of suspended sediment on fertilisation, larval survival and settlement in a scleractinian coral. *Marine Biology* **135(3)**:451–462 DOI 10.1007/s002270050645.

Graham NAJ, Nash KL. 2013. The importance of structural complexity in coral reef ecosystems. *Coral Reefs* **32(2)**:315–326 DOI 10.1007/s00338-012-0984-y.

Haas AF, Nelson CE, Rohwer F, Wegley-Kelly L, Quistad SD, Carlson CA, Leichter JJ, Hatay M, Smith JE. 2013. Influence of coral and algal exudates on microbially mediated reef metabolism. *PeerJ* **1(11)**:e108 DOI 10.7717/peerj.108.

Hadas E, Ilan M, Shpigel M. 2008. Oxygen consumption by a coral reef sponge. *Journal of Experimental Biology* **211(13)**:2185–2190 DOI 10.1242/jeb.015420.

Hallock P. 2005. Global change and modern coral reefs: new opportunities to understand shallow-water carbonate depositional processes. *Sedimentary Geology* **175(1–4)**:19–33 DOI 10.1016/j.sedgeo.2004.12.027.

Hoegh-Guldberg O. 1999. Climate change, coral bleaching and the future of the world's coral reefs. *Marine and Freshwater Research* **50(8)**:839–866 DOI 10.1071/MF99078.

Hoegh-Guldberg O, Mumby PJ, Hooten AJ, Steneck RS, Greenfield P, Gomez E, Harvell CD, Sale PF, Edwards AJ, Caldeira K, Knowlton N, Eakin CM, Iglesias-Prieto R, Muthiga N, Bradbury RH, Dubi A, Hatziolos ME. 2007. Coral reefs under rapid climate change and ocean acidification. *Science* **318(5857)**:1737–1742 DOI 10.1126/science.1152509.

Hubbard DK, Miller AI, Scaturo D. 1990. Production and cycling of calcium carbonate in a shelf-edge reef system (St. Croix, US Virgin Islands): applications to the nature of reef systems in the fossil record. *Journal of Sedimentary Research* **60(3)**:335–360 DOI 10.1306/212F9197-2B24-11D7-8648000102C1865D.

Hughes TP. 1994. Catastrophes, phase-shifts, and large-scale degradation of a Caribbean coral reef. *Science* **265(5178)**:1547–1551 DOI 10.1126/science.265.5178.1547.

Hughes TP, Rodrigues MJ, Bellwood DR, Ceccarelli D, Hoegh-Guldberg O, McCook L, Moltschwaniwskyj N, Pratchett MS, Steneck RS, Willis B. 2007. Phase shifts, herbivory, and the resilience of coral reefs to climate change. *Current Biology* **17(4)**:360–365 DOI 10.1016/j.cub.2006.12.049.

Hydes DJ, Aoyama M, Aminot A, Bakker K, Becker S, Coverly S, Daniel A, Dickson AG, Grosso O, Kerouel R, van Ooijen J. 2010. Recommendations for the determination of nutrients in seawater to high levels of precision and inter-comparability using continuous flow analysers. *GO-SHIP (Unesco/IOC). Available at http://agris.fao.org/agris-search/search.do?recordID=AV2012076378*.

Kennedy EV, Perry CT, Halloran PR, Iglesias-Prieto R, Schönberg CH, Wisshak M, Mumby PJ. 2013. Avoiding coral reef functional collapse requires local and global action. *Current Biology* **23(10)**:912–918 DOI 10.1016/j.cub.2013.04.020.

Koweek D, Dunbar RB, Rogers JS, Williams GJ, Price N, Mucciarone D, Teneva L. 2015. Environmental and ecological controls of coral community metabolism on Palmyra Atoll. *Coral Reefs* **34(1)**:339–351 DOI 10.1007/s00338-014-1217-3.

Kleypas JA, Buddemeier RW, Archer D, Gattuso JP, Langdon C, Opdyke BN. 1999. Geochemical consequences of increased atmospheric carbon dioxide on coral reefs. *Science* **284(5411)**:118–120 DOI 10.1126/science.284.5411.118.

Liu X, Byrne RH, Lindemuth M, Easley R, Mathis JT. 2015. An automated procedure for laboratory and shipboard spectrophotometric measurements of seawater alkalinity: Continuously monitored single-step acid additions. *Marine Chemistry* **174**:141–146 DOI 10.1016/j.marchem.2015.06.008.

Ludeman DA, Reidenbach MA, Leys SP. 2017. Correction: the energetic cost of filtration by demosponges and their behavioural response to ambient currents. *Journal of Experimental Biology* **220(24)**:4743–4744 DOI 10.1242/jeb.173849.

McGillis WR, Langdon C, Loose B, Yates KK, Corredor J. 2011. Productivity of a coral reef using boundary layer and enclosure methods. *Geophysical Research Letters* **38(3)**:1–5 DOI 10.1029/2010GL046179.

McMahon A, Santos IR, Cyronak T, Eyre BD. 2013. Hysteresis between coral reef calcification and the seawater aragonite saturation state. *Geophysical Research Letters* **40(17)**:4675–4679 DOI 10.1002/grl.50802.

McMurray SE, Stubler AD, Erwin PM, Finelli CM, Pawlik JR. 2018. A test of the sponge-loop hypothesis for emergent Caribbean reef sponges. *Marine Ecology Progress Series* **588**:1–14 DOI 10.3354/meps12466.

Middelburg JJ, Duarte CM, Gattuso J-P. 2005. *Respiration in coastal benthic communities. Respiration in aquatic ecosystems*. Oxford: Oxford University Press, 206–224.

Mintrop L, Pérez FF, González-Dávila M, Santana-Casiano JM, Körtzinger A. 2000. Alkalinity determination by potentiometry: intercalibration using three different methods. *Ciencias Marinas* **26(1)**:23–37 DOI 10.7773/cm.v26i1.573.

Murphy GN, Perry CT, Chin P, McCoy C. 2016. New approaches to quantifying bioerosion by endolithic sponge populations: applications to the coral reefs of Grand Cayman. *Coral Reefs* **35(3)**:1109–1121 DOI 10.1007/s00338-016-1442-z.

Newman MJ, Paredes GA, Sala E, Jackson JB. 2006. Structure of Caribbean coral reef communities across a large gradient of fish biomass. *Ecology Letters* **9(11)**:1216–1227 DOI 10.1111/j.1461-0248.2006.00976.x.

Odum HT, Hoskin CM. 1958. *Comparative studies on the metabolism of marine waters*. Vol. 5. Texas: Publications of the Institute of Marine Science, 16–46.

Paerl HW, Paul VJ. 2012. Climate change: links to global expansion of harmful cyanobacteria. *Water Research* **46(5)**:1349–1363 DOI 10.1016/j.watres.2011.08.002.

Patterson MR, Sebens KP, Olson RR. 1991. In situ measurements of flow effects on primary production and dark respiration in reef corals. *Limnology and Oceanography* **36(5)**:936–948 DOI 10.4319/lo.1991.36.5.0936.

Perry CT, Murphy GN, Graham NA, Wilson SK, Januchowski-Hartley FA, East HK. 2015. Remote coral reefs can sustain high growth potential and may match future sea-level trends. *Scientific Reports* **5(1)**:18289 DOI 10.1038/srep18289.

Perry CT, Murphy GN, Kench PS, Smithers SG, Edinger EN, Steneck RS, Mumby PJ. 2013. Caribbean-wide decline in carbonate production threatens coral reef growth. *Nature communications* **4(1)**:1402 DOI 10.1038/ncomms2409.

Perry CT, Spencer T, Kench PS. 2008. Carbonate budgets and reef production states: a geomorphic perspective on the ecological phase-shift concept. *Coral Reefs* **27(4)**:853–866 DOI 10.1007/s00338-008-0418-z.

Porter JW, Meier OW. 1992. Quantification of loss and change in Floridian reef coral populations. *American Zoologist* **32(6)**:625–640 DOI 10.1093/icb/32.6.625.

Redfield AC. 1963. The influence of organisms on the composition of seawater. *The sea* **2**:26–77.

Roche DG, Binning SA, Bosiger Y, Johansen JL, Rummer JL. 2013. Finding the best estimates of metabolic rates in a coral reef fish. *Journal of Experimental Biology* **216(11)**:2103–2110 DOI 10.1242/jeb.082925.

Shaw EC, McNeil BI, Tilbrook B. 2012. Impacts of ocean acidification in naturally variable coral reef flat ecosystems. *Journal of Geophysical Research: Oceans* **117**:C03038 DOI 10.1029/2011jc007655.

Shaw EC, Phinn SR, Tilbrook B, Steven A. 2014. Comparability of slack water and Lagrangian flow respirometry methods for community metabolic measurements. *PLOS ONE* **9(11)**:e112161 DOI 10.1371/journal.pone.0112161.

Shaw EC, Phinn SR, Tilbrook B, Steven A. 2015. Natural in situ relationships suggest coral reef calcium carbonate production will decline with ocean acidification. *Limnology and Oceanography* **60(3)**:777–788 DOI 10.1002/lno.10048.

Silbiger NJ, Donahue MJ. 2015. Secondary calcification and dissolution respond differently to future ocean conditions. *Biogeosciences* **12(2)**:567–578 DOI 10.5194/bg-12-567-2015.

Smith SV, Key GS. 1975. Carbon dioxide and metabolism in marine environments. *Limnology and Oceanography* **20(3)**:493–495 DOI 10.4319/lo.1975.20.3.0493.

Takeshita Y, McGillis W, Briggs EM, Carter AL, Donham EM, Martz TR, Price NN, Smith JE. 2016. Assessment of net community production and calcification of a coral reef using a boundary layer approach. *Journal of Geophysical Research: Oceans* **121(8)**:5655–5671 DOI 10.1002/2016JC011886.

Webb AE, Van Heuven SMAC, De Bakker D, Van Duyl FC, Reichart G-J, De Nooijer Lennart LJ. 2017. Combined effects of experimental acidification and eutrophication on reef sponge bioerosion rates. *Frontiers in Marine Science* **4**:311 DOI 10.3389/fmars.2017.00311.

Wild C, Huettel M, Klueter A, Kremb SG, Rasheed MY, Jørgensen BB. 2004. Coral mucus functions as an energy carrier and particle trap in the reef ecosystem. *Nature* **428(6978)**:66–70 DOI 10.1038/nature02344.

Wisshak M, Schönberg CHL, Form A, Freiwald A. 2013. Effects of ocean acidification and global warming on reef bioerosion—lessons from a clionaid sponge. *Aquatic Biology* **19(2)**:111–127 DOI 10.3354/ab00527.

Wood BL. 1967. Geology of the Cook Islands. *New Zealand Journal of Geology and Geophysics* **10(6)**:1429–1445 DOI 10.1080/00288306.1967.10423227.

Yates KK, Halley RB. 2003. Measuring coral reef community metabolism using new benthic chamber technology. *Coral Reefs* **22(3)**:247–255 DOI 10.1007/s00338-003-0314-5.

Yates KK, Zawada DG, Smiley NA, Tiling-Range G. 2017. Divergence of seafloor elevation and sea level rise in coral reef ecosystems. *Biogeosciences* **14(6)**:1739–1772 DOI 10.5194/bg-14-1739-2017.